Transient electromagnetic simulation and thermal analysis of the DC-biased AC quadrupole magnet for CSNS/RCS

SUN Xian-Jing(孙献静)[1)] DENG Chang-Dong(邓昌东) KANG Wen(康文)

Institute of High Energy Physics, Chinese Academy of Sciences, Beijing 100049, China

Abstract: Due to the large eddy currents at the ends of the quadrupole magnets for CSNS/RCS, the magnetic field properties and the heat generation are of great concern. In this paper, we take transient electromagnetic simulation and make use of the eddy current loss from the transient electromagnetic results to perform thermal analysis. Through analysis of the simulated results, the magnetic field dynamic properties of these magnets and a temperature rise are achieved. Finally, the accuracy of the thermal analysis is confirmed by a test of the prototype quadrupole magnet of the RCS.

Key words: CSNS, RCS, transient electromagnetic simulation, thermal analysis

PACS: 29.20.D-, 41.85.Lc, 07.55.Db **DOI:** 10.1088/1674-1137/36/5/011

1 Introduction

The Rapid Cycling Synchrotron (RCS) of the China Spallation Neutron Source (CSNS) [1–3], which is operated at a frequency of 25 Hz, has 24 dipoles and 48 quadrupoles. The quadrupole magnets (QM), which are excited by the direct current (DC) biased alternating current (AC), are made of coils, laminated steel sheets (iron core), insulation material between the sheets and stainless steel (SS) end plates. Since the changing magnetic fields lead to large eddy currents in the iron core and the SS end plates, the magnetic field quality of the good regions will be greatly affected [4]. To hold the characteristics of these magnets, which include the change in gradient and the retarded time, and so on, we try to take the transient electromagnetic simulation [5–7]. Furthermore, the eddy currents can also cause heat loss and a high temperature rise in these magnets. Since the excess temperature rise would damage the adhesive resin in the core end area, the evaluation of the temperature rise of these magnets plays an important role. In order to reduce the temperature rise, many measures, including slit arrangements on the core and multi-conductor coils, need to be adopted [8, 9]. So, the credible thermal analysis of these magnets is the basis of the magnet design scheme.

Heat generation due to AC operation occurs for three reasons. The first is the eddy currents in the sheets which flow along the sheet surfaces, the second is the eddy currents which are induced in the SS end plates, and the third is iron loss due to hysteresis and eddy currents in the sheets flowing in the thin cross sections. The first and second ones are found to be the major causes of temperature rise. The iron cores of these magnets are made of 0.5 mm thick electrical steel sheets and little eddy currents can flow along the sheets. In the end areas, the magnetic fields flow through the sheets and generate the intense eddy currents.

In this paper, 3D transient electromagnetic simulation and thermal analysis are used to calculate the dynamic electromagnetic field and the temperature distribution. The former is done by ELEKTRA TR and the latter by TEMPO ST of OPERA [10] with basic material constants. The analysis results are confirmed by the experimental test of the prototype QM.

Received 3 August 2011

1) E-mail: :sunxj@ihep.ac.cn

2 Transient electromagnetic simulation

Transient electromagnetic simulation is a valid method to seize the electromagnetic fields at any time. The electromagnetic fields of QM are excited by the DC-biased AC. The current equation is:

$$I = I_{\rm DC} + I_{\rm AC}\sin(2\pi f t), \tag{1}$$

where the frequency $f = 25$ Hz, $I_{\rm DC}$ and $I_{\rm AC}$ are the direct current and the amplitude of the alternating current, respectively.

The magnetic field of QM belongs to the low-frequency electromagnetic field. It is described by the quasi-static limit of Maxwell's equations, which excludes the displacement current and the velocity of media with respect to the field. In this limit, Maxwell's equations have the form:

$$\nabla \times \boldsymbol{H} = \boldsymbol{J}, \tag{2}$$

$$\nabla \times \boldsymbol{E} = -\frac{\partial \boldsymbol{B}}{\partial t}, \tag{3}$$

$$\nabla \cdot \boldsymbol{B} = 0, \tag{4}$$

where $\boldsymbol{H}$ is the magnetic field strength and $\boldsymbol{B}$ is the flux density. The relation between electric field strength $\boldsymbol{E}$ and current density $\boldsymbol{J}$ is:

$$\boldsymbol{J} = \sigma \boldsymbol{E}, \tag{5}$$

where σ is the conductivity of the material.

From the above equations, the changing magnetic field in the iron core of QM can produce the eddy current and at the same time the eddy current also prevents the magnetic field from changing. Therefore, both the heat generation and the magnetic field lag about QM are regarded greatly.

2.1 The 3D model

Because of the magnet symmetry, only a 1/8 QM model is built with end chamfering and slot cuts [5]. As shown in Fig. 1, part A is the laminated core and part B is the SS end plate. Four coils with the type of the tangential constant perimeter ends (CPE) conductor are part C [10]. In order to improve the precision of the 3D simulation, different mesh sizes are used in different regions according to the effect on the good region. Moreover, the coil excitation is the circuit element with AC, DC current source and conductor winding, not the Biot-Savart current source. The parameters of the QM are listed in Table 1.

Table 1. The QM parameters.

magnet	aperture/mm	turn	$I_{\rm DC}$/A	$I_{\rm AC}$/A
QM	308	24	914.8	652

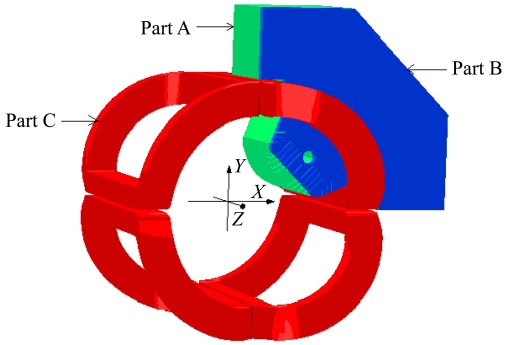

Fig. 1. The 3D simulation model.

2.2 Parameters

When the transient electromagnetic analysis of QM is taken, the magnetic and electric parameters of the materials need to be defined. The core is made of laminated steel of type J23-50, produced by Wuhan Iron and Steel Corporation. Conductivity in the laminated direction is assumed to be zero and the packing factor is 98%. The SS end plate is non-magnetic but conductive material. The material conductivities of the iron core and the SS end plate are listed in Table 2.

2.3 Analysis results

From the transient electromagnetic calculation, we obtain the distributions of the eddy currents of QM as shown in Fig. 2(a). The arrows point to the direction of the eddy currents and the size of the arrows shows the magnitude of the eddy currents. Figs. 2(b) and (c) show that the eddy currents can be reduced dramatically by slot cuts at the ends of the QM.

Table 2. Material constants.

parameters	parts	conductivity	thermal conductivity
unit		S/mm	W/(mm/K)
iron core	laminate direction	0	5.4E-03
	non-laminate direction	3571.43	0.0368
SS end plate		1428.57	0.0146

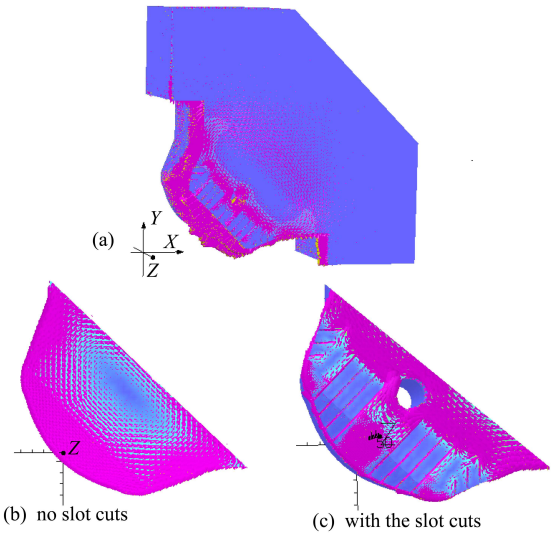

Fig. 2. The eddy current distribution of the 1/8 model (a), and the poletip with no slot cuts (b) and with slot cuts (c).

The simulated field gradient G versus time t of the QM in the good region is given in Fig. 3(b), which is compared with the exciting current I shown in Fig. 3(a). Due to the different currents and the eddy currents induced by the changing currents on the pole tips of QM, the allowed harmonic field errors are affected greatly, as shown in Fig. 3(c). The curves are the errors of b6 (the solid circle curve), b10 (the solid triangle curve), and b14 (the vacant circle curve). It is shown that the harmonic b6 changes obviously at the highest current, while b10 changes at the lowest current. The allowed harmonics in the good region lie on the magnetic field distribution of the QM poletips.

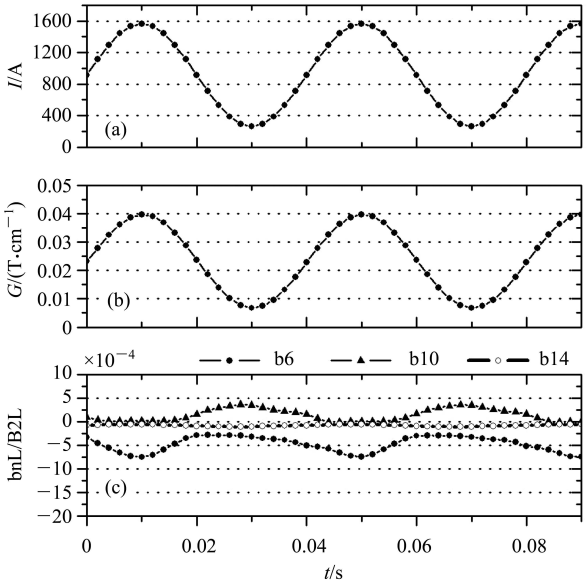

Fig. 3. The relation between the time and the magnetic field.

Changes in these harmonics are caused by the local saturation and the eddy currents of the QM poletips.

Due to the effect of the eddy currents, the waveform of the magnetic field deforms slightly and lags behind the exciting current, as shown in Fig. 4. The solid circle curve is the waveform of the currents and the vacant circle curve is of the gradient integral of the magnetic field. In order to show the delay clearly, the linear parts of the waveforms are enlarged in Fig. 4(b). Through analyses of both the magnetic field and the excited current curves, the delay time was achieved. The delay time is 0.25 ms and the opposite phase angle lags 2.25°. Owing to the delay, the excited currents of QM aren't synchronous with the magnetic fields. In order to keep up with the magnetic fields, the lattice injection should be deferred at the same time when the excited currents of QM reach the maximum values.

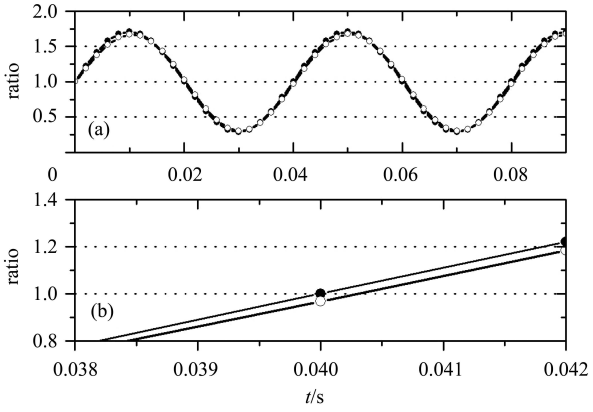

Fig. 4. The retarded time.

3 Thermal analysis

Three-dimensional thermal fields can be represented using a single scalar potential (T). Physically, T is the usual temperature field. The heat source density, q, is given by:

$$\nabla\cdot\kappa\ \nabla T=-q, \tag{6}$$

where κ is the thermal conductivity.

The boundary conditions about QM are described in the following.

$$\begin{cases}\kappa\dfrac{\partial T}{\partial n}=q\cdot n=0\\ q\cdot n=h(T-\alpha)\end{cases}, \tag{7}$$

where α is the ambient temperature, h is the heat-transfer coefficient and n is the normal unit vector to the surface being considered.

The heat source density can be specified using the element heat, which is from the power loss of QM. Furthermore, the evaluation of the temperature rise is related to the heat transfer coefficient of the magnet surface.

3.1 The thermal model

The thermal model of QM includes the laminated steel sheets and the SS end plates. In order to get a reasonable evaluation of the temperature rise, the mesh sizes of the thermal model are different from the previous model. Each part of the model has the same-sized finite element.

As listed in Table 2, the thermal constants are different everywhere. In the laminated direction, all the steel sheets are pasted with epoxy resin and the heat quantity conducts through the epoxy resin between the sheets. The conductivity is 5.4E-03 W/(mm/K). The other direction of the iron core is 0.0368 W/(mm/K). The thermal conductivity of the SS end plates is 0.0146 W/(mm/K). Heat radiates from the surface of the magnet and the heat transfer coefficient is assumed to be 1.4E-5 W/(K/mm^2). Using these constants, we conduct the thermal analysis of QM.

3.2 Analysis results

The heat loss of each finite element, which is calculated by the transient electromagnetic simulation, is put into the thermal analysis. It deals with the virtual value of the whole period. Subsequently, the virtual value of the loss is placed into the opposite element of the thermal model. Finally, the thermal calculation is done by TEMPO ST of OPERA [10].

The simulated result shows that the maximal temperature of QM is 137 ℃ when the ambient temperature is assumed to be 20 ℃, as shown in Fig. 5. Furthermore, the maximal temperature measured is more than 130 ℃, which is similar to the calculated result.

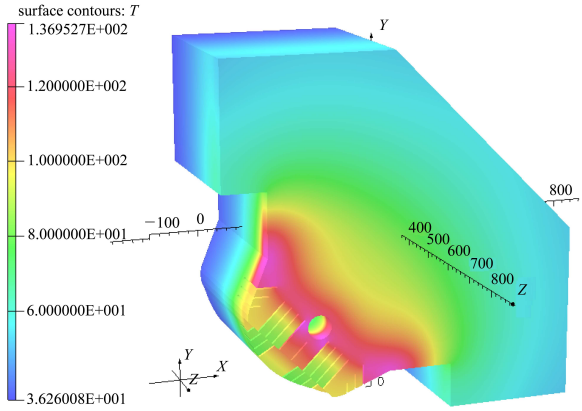

Fig. 5. Temperature distribution with the SS end plate.

4 Conclusion

In the process of transient electromagnetic simulation, the circuit element current source is successfully used to deal with the DC-biased AC exciting current. Due to the effect of the eddy current, the waveform of the magnetic field in the good region deforms slightly and lags behind the exciting current. The end slot cuts of the magnet can reduce the eddy current effectively. Finally, the eddy loss from the transient electromagnetic simulation is put into the thermal analysis and the calculated result is in good agreement with the measured data.

The authors would like to thank Prof. Yin Zhao-Sheng for his guidance and all the colleagues of the Magnet Group.

References

1 WEI J, FU S N, TANG J Y et al. Chin. Phys. C (HEP & NP), 2009, **33**(11): 1033
2 WANG S, FANG S X, FU S N et al. Chin. Phys. C (HEP & NP), 2009, **33** (Suppl. Ⅱ): 1
3 Spallation Neutron Source: The Next-generation Neutron Scattering Facility for the United States. Department of Energy, 1998. SNS website: http://www.sns.gov
4 Tani N et al. IEEE Transactions on Applied Superconductivity, 2004, **14**(2): 421
5 Abe M et al. Transient Electromagnetic Analysis and Thermal Design on the Magnet of 3-GeV Synchrotron. Proceedings of EPAC08, Genoa, Italy, 2332
6 Jay A P, Sykulski J K, Lepau1 S. IEEE Transactions on Magnetics, 1998, **34**(5): 3182
7 ZHOU J X, LI L et al. Nuclear Instruments and Methods in Physics Research A, 2010, **624**: 549
8 DENG C D, CHEN F S, SUN X J et al. Chin. Phys. C (HEP & NP), 2008, **32**(Suppl. Ⅰ): 71 (in Chinese)
9 Tani N et al. IEEE Transactions on Applied Superconductivity, 2004, **14**(2): 409
10 Opera-3D Reference, http://www.vectorfields.com